

Analysis of Fundamental Data Rates in Rician Fading Wireless Channels Using Small Limit Argument Approximation

Abstract—The rate of information transmission in wireless communication has dramatically evolved over the last decade. However, due to multipath propagation, the data rate is not constant, even though a reasonably stable data rate is essential for effective wireless transmission. Historically, various fading system models have been employed to analyze and demonstrate the dynamics of remote communication channels. Recent research focuses on SISO wireless communication systems operating under Rician fading conditions. By employing small-limit argument approximations, researchers can evaluate channel capacity with greater accuracy, particularly in scenarios characterized by low signal-to-noise ratios (LSNR). This approach facilitates the development of analytical methods for calculating channel capacities, offering valuable insights into system performance under challenging conditions. The analysis delves into how channel capacity responds to variations in real-time signal-to-noise ratio (SNR), also known as instantaneous SNR, the Rician factor, and the overall power of fading. This comprehensive examination provides new perspectives on the performance of wireless communication systems under these conditions. The SISO model also considers the impact of the Rician factor and the overall power of Rician fading. According to the research, the capacity of the channel increases significantly with the rise of real-time SNR when using the small-limit argument approximation. Additionally, the study explores the highest possible channel capacity for the proposed system under this approximation.

Index Terms—Channel Capacity, Rician Fading, SISO, SNR, Wireless Communication

I. INTRODUCTION

In the rapidly evolving field of wireless communications, the ability to reliably transmit data across various channels is paramount. As technologies advance and the demand for higher data rates increases, understanding channel capacity becomes crucial for optimizing network performance and enhancing the user experience. Channel capacity, a fundamental concept in information theory, represents the maximum rate at which data can be reliably transmitted across a communication channel with minimal loss [1]. This metric is essential for both the design and analytical evaluation of wireless communication systems.

Wireless channels are often subjected to various types of fading, which can severely impact communication system performance [2]. Among these, Rician and Rayleigh fading are predominant models used to represent real-world conditions where multipath scattering and line-of-sight components are present. Rician fading, in particular, is significant for environments where a direct line of sight between the transmitter and receiver exists alongside scattered paths. The dual nature of Rician fading makes it a challenging yet essential model for improving channel capacity estimations under non-ideal conditions.

Despite considerable advances, accurately estimating channel capacity in Rician fading environments, especially under LSNR conditions, remains a complex challenge. Previous studies have often focused on high-SNR regimes or simplified models that do not fully capture the variability introduced by Rician fading. The current research aims to bridge this gap by focusing on small-limit argument approximations—a method less explored in current literature but promising for LSNR conditions.

This paper presents a comprehensive analysis of channel capacity in SISO wireless systems under Rician fading. By employing small-limit argument approximations, novel insights are offered into how channel capacity can be optimized despite the adverse effects of fading. This study advances the understanding of channel behavior in LSNR conditions and contributes to methodologies that could influence future designs and optimizations of wireless communication frameworks.

The following sections will explore the background of channel capacity studies, detail the methodological approach using small-limit argument approximations, present the results of empirical investigations, and discuss the implications of the findings for both theory and practical applications in wireless communications.

II. LITERATURE REVIEW

The concept of information-theoretic channel capacity and the fundamental formats of communication across remote frameworks were initially proposed in reference [3]. Subsequently, the channel's information capacity in relation to various dispersions was investigated through numerous exhaustive tests. Over time, wireless architectures have progressed from the SISO model to a range of specialized wireless frameworks. In the SISO configuration, both the transmitting and receiving units are equipped with a single antenna each.

In reference [4], researchers performed analyses on channel capacities for SISO and multiple-input and multiple-output (MIMO) systems, tailoring their investigations to the unique properties of each system type. Studies have incorporated a variety of statistical distributions, such as constant dispersion, Gaussian conveyance, and Chi-square, to examine SISO channel capacity [5]. Additional work [6] evaluated the performance of SISO alongside MIMO and single-input multiple-output (SIMO) systems, providing insights into how these frameworks perform under Rayleigh fading conditions. This was further detailed in the analysis of channel capacities for both MIMO and SISO channels [7]. The study of signal behavior in these systems often involves Rician, Rayleigh, and Nakagami-M distributions, with the Rayleigh distribution being particularly notable for representing the most challenging fading scenarios [8], [9].

The Rician distribution offers a broader application spectrum, making it suitable for modeling various fading scenarios. Rician fading occurs during signal transmission to the receiver, involving at least one variable path and typically including a line-of-sight (LOS) component. In cases where the LOS component is absent, Rayleigh fading becomes significant within the context of Rician fading. Under such conditions, the Rician distribution accounts for the amplitude variations caused by Rician fading and effectively supersedes the Rayleigh distribution.

Modern wireless communication frameworks are designed to dynamically modify transmission parameters based on real-time channel measurements. One critical measurement is the Rician factor k , associated with the line-of-sight component, which is essential for evaluating fading characteristics that influence bit error rate, spectral efficiency, level crossing rate, and average fade duration, among others. These elements collectively influence the configuration of communication systems. In reference [10], research delves into the performance analysis of Rician fading channels through the use of non-linear adjustment techniques, including memory schemes, analyzed using the Simulink tool. Particularly for satellite communications, the Rician distribution is favored over other models due to its suitability in such contexts [11].

In wireless communication systems, the performance of the transmission medium's link quality is crucial. Insufficient quality of the transmission medium can lead to signal degradation between the transmitter and receiver. Understanding link quality is fundamental to establishing a robust commu-

nication channel. Various quality factors are used to describe and assess end-to-end quality, including SNR [12] and delay spread [13]. The Rician factor k , a key metric in the Rician distribution, significantly influences link quality assessment. This factor, representing the amplitude of the received signal envelope described by the Rician distribution, quantifies the ratio between the powers of the LOS and diffuse components. It is instrumental in evaluating LOS quality and overall link integrity. The value of the Rician factor also indicates fading severity, with $k = 0$ depicting extreme Rayleigh fading and $k = \infty$ indicating no fading [14].

The Rayleigh distribution is widely recognized as the predominant signal model in remote communications, primarily due to its ability to accurately represent severe fading conditions. However, when a line-of-sight component is present, the Rician distribution is better suited and demonstrates superior performance [15]. This study focuses on the Rician fading channel for analyzing channel capacity. The Rician distribution is adaptable for use with both large-limit and small-limit argument approximations. This research includes a detailed examination of the channel capacity in SISO wireless communication frameworks under the influence of Rician fading.

The primary aim of this research is to calculate the channel capacity of SISO wireless communication systems subjected to Rician fading, specifically using the small-limit argument approximation. Additionally, this study seeks to validate the accuracy of the derived equations and assess the practical channel capacities achieved under these conditions. The results and interpretations of these investigations are thoroughly presented.

III. PROPOSED SISO ARCHITECTURE

Rician fading, also known as a stochastic model due to radio dispersion, occurs when the transmitted signal is received by the receiver through multiple paths. This scenario arises when there is a line-of-sight signal or several strong reflected signals that are more intense than others. The Rician distribution characterizes the total amplitude gain in Rician fading [16].

Throughout the extensive history of wireless communications, various channel models have been proposed to describe the characteristics of signal propagation, including the timing of multipath signals, depending on the structure and operating conditions. The Rician fading model was first introduced by Stephen O. Rice to assess the Rician distribution. In a Rayleigh fading environment, when a strong stationary path is present, the fading is termed Rician fading, also known as small-scale fading [17].

The probability distribution function (PDF) of Rician fading is described in [18] by

$$f(x) = \frac{2(k+1)x}{\Omega} \exp\left(-k - \frac{(k+1)x^2}{\Omega}\right) I_0\left(\frac{2}{\Omega} \sqrt{k(k+1)}x\right);$$

$$\Omega \geq 0 \quad (1)$$

where I_0 denotes the zeroth-order modified Bessel function of the first kind. The Rician fading model is characterized by

two key parameters [19]. The first parameter, k , known as the Rician factor, quantifies the relationship between the power of the direct path and the scattered paths [20]:

$$k = \frac{v^2}{2\sigma^2}$$

The second parameter, Ω , represents the total power of both direct and scattered paths:

$$\Omega = v^2 + 2\sigma^2$$

The amplitude gain of the fading channel at the receiver can be expressed using the following two equations, which incorporate the two parameters [21]:

$$v^2 = \frac{k}{1+k}\Omega$$

$$\sigma^2 = \frac{\Omega}{2(1+k)}$$

In a SISO wireless communication framework, the system is configured with a single antenna at both the transmitter and receiver for sending and receiving signals, respectively [22].

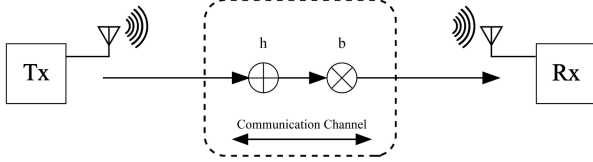


Fig. 1. Proposed system architecture for SISO framework.

The architectural setup of the SISO framework is illustrated in Figure 1. For analytical purposes, Q_t is defined as the transmitted signal power. It is also assumed that the receiver is affected by additive white Gaussian noise (AWGN), which is typical in such systems. The communication process is further influenced by Rician fading. According to the model described in [23], the expression for the received signal Rx can be represented as:

$$Rx = h * Tx + b \quad (2)$$

Here, h is a vector that characterizes channel gains from the transmitter to the receiver, T_x represents the transmitted signal, and b is another vector representing zero-mean AWGN. In the SISO communication framework, Shannon's channel capacity, which denotes the maximum achievable rate between the transmitted and received signals, is expressed in [24] as:

$$C = B \log_2(1 + p) \quad (3)$$

where $p = \frac{Q_t}{N}$ defines the ratio of the transmitted signal power to the noise power, and B represents the system's bandwidth. The power constraint in the channel is denoted by $Q_t = \mathbb{E}\{|x|^2\}$, where $\mathbb{E}\{\cdot\}$ is the expected value operator, and is calculated based on the PDF of the channel gain, denoted as h [22], [25]. In the context of low signal-to-noise ratio (LSNR), using the small-limit argument approximation for channel capacity, as described in [26], it is assumed that the

zeroth-order modified Bessel function of the first kind, $I_0 \approx 1$. Following this assumption, the PDF expressed in equation 1 simplifies to:

$$f(x) = \frac{2(k+1)x}{\Omega} \exp\left(-k - \frac{(k+1)x^2}{\Omega}\right); \quad \Omega \geq 0 \quad (4)$$

In the subsequent section, the channel capacity of the proposed SISO system is derived.

IV. DERIVATION OF CHANNEL CAPACITY

This chapter focuses on deriving the Rician-fading SISO wireless channel capacity, particularly under conditions of low signal-to-noise ratio (LSNR). Channel capacity is determined using Equation 3:

$$C = \int_0^\infty f(x) \log_2(1 + px) dx \quad (5)$$

By integrating Equation 4 into Equation 5, the channel capacity for LSNR scenarios is calculated as follows:

$$C = \int_0^\infty \frac{2(k+1)x}{\Omega} \exp\left(-k - \frac{(k+1)x^2}{\Omega}\right) \log_2(1 + px) dx \quad (6)$$

To further clarify and confirm the results obtained from Equation 6, Mathematica [27], a tool renowned for its capabilities in advanced computing, was employed. This facilitated a thorough investigation of the channel capacity within this framework under LSNR conditions. The computation using Equation 6 produces the final measure of channel capacity for LSNR. The condition for convergence is provided as:

$$C_{LowSNR} = \left(e^{-\frac{1+k+k\Omega p^2}{\Omega p^2}} \left(\begin{array}{l} 2\pi \operatorname{Erfi}\left[\frac{\sqrt{1+k}}{\Omega} \frac{1}{p}\right] - 2 \operatorname{Ei}\left[\frac{1+k}{\Omega p^2}\right] \\ -2 \log\left[\frac{1+k}{\Omega}\right] + \log\left[\frac{1+k}{\Omega p^2}\right] \\ + 4 \log[p] - \log\left[\frac{\Omega p^2}{1+k}\right] \end{array} \right) \right) / 4 \log[2]$$

$$\text{If } \operatorname{Re}[k] \neq 0 \text{ and if } \operatorname{Re}\left[\frac{1+k}{\Omega}\right] > 0 \quad (7)$$

Here, $\operatorname{Erfi}(x)$ represents the "imaginary error function," and the exponential integral Ei represents the "special function" on the complex plane.

V. RESULTS AND DISCUSSION

The chapter on results and discussion is divided into two main sections. The first section explores the influence of real-time SNR on the probability distribution function (PDF) of Rician fading. The second section evaluates channel capacity in relation to real-time SNR. This analysis investigates how variations in the Rician factor k and the total power Ω impact channel capacity. Each parameter is examined independently to assess its effect on channel capacity within the framework of the small-limit argument approximation, as outlined in this chapter.

A. Effect of the real-time SNR on PDF

The amplitude of Rician fading is measured using both small-limit and large-limit argument approximations. The Bessel function (I_0) is present in Rician fading when using the large-limit argument approximation and the PDF given in Equation 1. However, in the small-limit argument approximation, the Bessel function (I_0) is approximated as $(I_0) \approx 1$, leading to the PDF of the Rician distribution as shown in Equation 4.

The behavior of the PDF is analyzed under the large-limit argument approximation for specific values of k and Ω . This method is relevant to scenarios characterized by high SNR, where the signal power significantly exceeds the noise power, defining high SNR conditions.

Figure 2 demonstrates that the amplitude of the PDF increases logarithmically with real-time SNR, then declines and stabilizes. The maximum amplitude of the PDF under the large-limit argument approximation is observed at 0.350019. Similarly, the amplitude of the PDF for Rician fading is examined under the small-limit argument approximation.

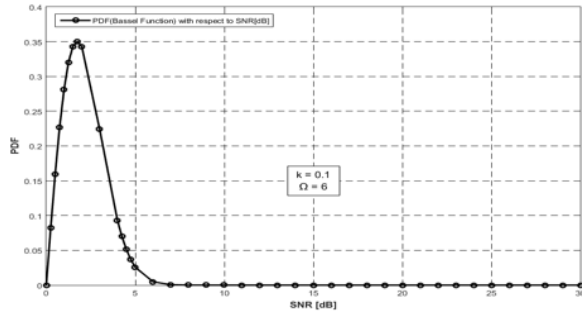


Fig. 2. Effect of the real-time SNR over PDF in large limit argument approximation when $k = 0.1$ and $\Omega = 6$.

The small-limit argument approximation corresponds to the LSNR regime, where the signal is lower than the noise. In Figure 3, it is shown that the highest amplitude of the PDF is 0.331163.

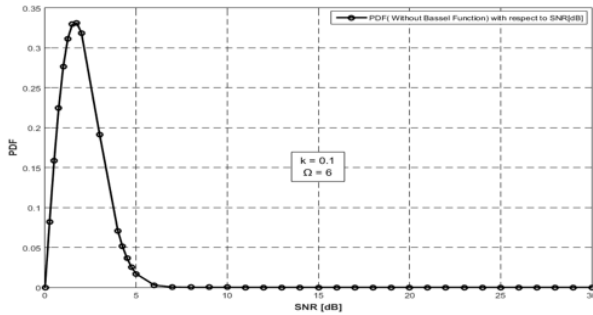


Fig. 3. Effect of the real-time SNR over PDF in small limit argument approximation when $k = 0.1$ and $\Omega = 6$.

The PDF of the Rician distribution is compared for both small-limit and large-limit argument approximations. Figure

4 illustrates that the amplitude of Rician fading in the large-limit approximation is higher than in the small-limit argument approximation.

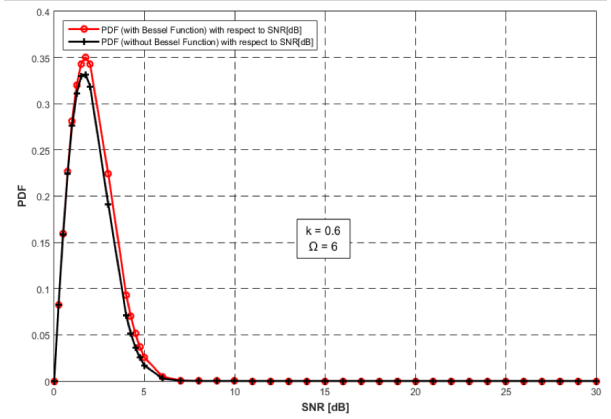


Fig. 4. Effect of the real-time SNR over PDF in large and small limit argument approximation when $k = 0.6$ and $\Omega = 6$.

B. Channel Capacity Vs. the real-time SNR

This study initially explores the influence of real-time SNR on channel capacity, particularly under LSNR conditions. The effects are illustrated in Figure 5, which displays the relationship between channel capacity and real-time SNR in LSNR scenarios with $k = 0.1$ and $\Omega = 1$.

The validity of Equation 7, derived from Equation 6, is confirmed by comparing their outcomes under the same parameters. As shown in Figure 5, the results from both equations align perfectly, confirming the accuracy of the derivation. The evaluation covers a range of real-time SNR values from 1 to 30 dB.

Figure 5 also depicts the growth in channel capacity of Rician fading within the SISO framework as real-time SNR increases. Specifically, at an SNR of 1 dB, the channel capacity is approximately 0.763045 bits/second/hertz (bps/Hz), progressively increasing to 4.07612 bps/Hz at an SNR of 30 dB.

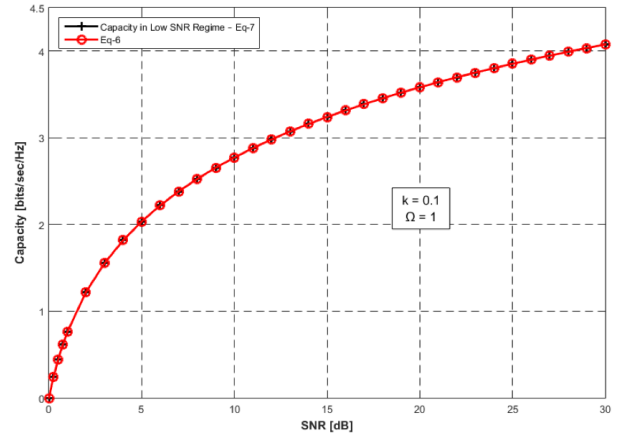


Fig. 5. Effect of the real-time SNR on channel capacity in LSNR.

Next, the behavior of channel capacity in the SISO model is analyzed by varying the Rician factor k from 0.1 to 0.3. In this scenario, the total power of the Rician fading model Ω is set to 1. Three different channel capacity behaviors are observed for the three different values of k . Through this analysis, more efficient channel capacities are identified for each value of the Rician factor.

As illustrated in Figure 6, there is a consistent increase in channel capacities across all three scenarios as real-time SNR increases. The maximum channel capacity reaches 4.07612 bps/Hz of 0.1. At the same SNR level, the channel capacity with a Rician factor k of 0.2 is slightly lower, recorded at 3.63968 bps/Hz . Meanwhile, with a Rician factor k of 0.3, the channel capacity at the same SNR is 3.25301 bps/Hz , marking the third highest in this evaluation.

To summarize, the highest channel capacity is found when the Rician factor k is 0.1 and the total power of the Rician fading Ω is 1.

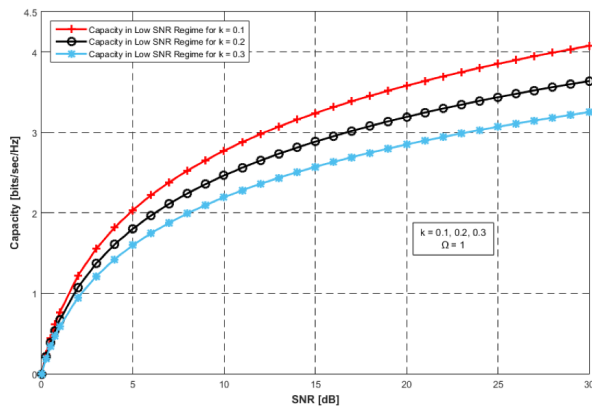


Fig. 6. Effect of the real-time SNR on channel capacity when $k = 0.1, 0.2, 0.3$ and $\Omega = 1$.

The behavior of channel capacity in the SISO model is also analyzed for real-time SNR by varying the total power of the Rician model. The total power Ω is considered at values of 1, 3, and 5, while the Rician factor k is set to 0.1. Three different channel capacity outcomes are observed for the three different values of Ω . Through this analysis, the more efficient channel capacities are identified for each value of total power.

As seen in Figure 7, all three channel capacities increase with respect to real-time SNR. The highest channel capacity is 4.07612 bps/Hz at an SNR of 30 dB when $\Omega = 1$. The second highest channel capacity is 4.76255 bps/Hz at an SNR of 30 dB when $\Omega = 3$. Finally, the highest channel capacity of 5.08624 bps/Hz is found at an SNR of 30 dB when $\Omega = 5$, which is the largest channel capacity among the three.

In conclusion, among the three different channel capacities for Ω , the most efficient channel capacity is found when the total power of the Rician model Ω is 5 and the Rician factor is $k = 0.1$.

VI. CONCLUSION AND FUTURE WORK

This thesis investigates the channel capacity in LSNR for the Rician-fading SISO wireless channel. The derivation of

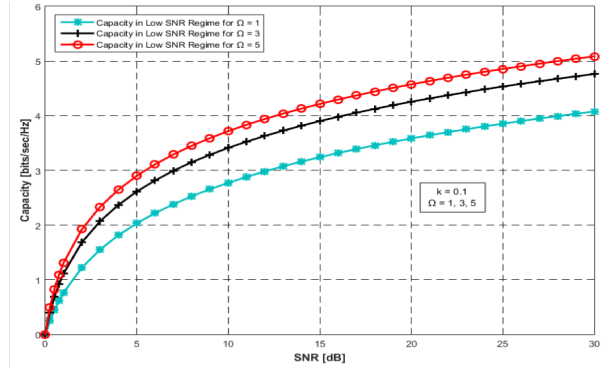


Fig. 7. Effect of the real-time SNR on channel capacity in LSR when $k = 0.1$ and $\Omega = 1, 3, 5$.

a novel logical expression for the channel capacity in LSNR for this framework using small-limit argument approximations is presented. The study conducts thorough investigations into channel capacity for LSNR. The values of the Rician factor k and total power Ω are examined for the SISO model, and the estimator yielded highly satisfactory results for meaningful values of these parameters. It is observed that channel capacity performance in LSNR increases with real-time SNR within the framework. Due to the small-limit argument approximation, channel capacity exhibits a logistic increase with respect to both the Rician factor and total power. The highest channel capacity in LSNR is achieved when $k = 0.1$ and $\Omega = 0.5$, indicating the optimal configuration for this proposed system. The primary objective of this research was to develop novel equations for channel capacity using the small-limit argument approximation, making a significant contribution to wireless communication system models.

This research focuses on the SISO wireless communication channel, utilizing the Rician distribution model. The derived equations for small-limit argument approximation are novel, and their accuracy is validated. In future work, channel capacity could be measured in the high SNR regime using the SISO model. Given the similarities between SISO and SIMO system models, particularly the multiple receivers in SIMO, the equations derived in this research could be adapted for the SIMO system model. This would allow for an analysis of capacity performance in a Rician-fading SIMO wireless channel under both LSNR and high SNR conditions.

REFERENCES

- [1] Y. Xiong, F. Liu, Y. Cui, W. Yuan, T. X. Han, and G. Caire, "On the fundamental tradeoff of integrated sensing and communications under gaussian channels," *IEEE Transactions on Information Theory*, vol. 69, no. 9, pp. 5723–5751, 2023.
- [2] P. Yadav, S. Kumar, and R. Kumar, "A comprehensive survey of physical layer security over fading channels: Classifications, applications, and challenges," *Transactions on Emerging Telecommunications Technologies*, vol. 32, no. 9, p. e4270, 2021.
- [3] L. Yang, J. Yang, W. Xie, M. O. Hasna, T. Tsiftsis, and M. D. Renzo, "Secrecy performance analysis of ris-aided wireless communication systems," *IEEE Transactions on Vehicular Technology*, vol. 69, no. 10, pp. 12 296–12 300, 2020.

- [4] D. Fernandes, F. Cercas, R. Dinis, and P. Sebastião, "Estimating the performance of mimo sc-fde systems using siso measurements," *Applied Sciences*, vol. 10, no. 21, 2020. [Online]. Available: <https://www.mdpi.com/2076-3417/10/21/7492>
- [5] M. Saad, J. Palicot, F. Bader, A. C. A. Ghouwayel, and H. Hijazi, "A novel index modulation dimension based on filter domain: Filter shapes index modulation," *IEEE Transactions on Communications*, vol. 69, no. 3, pp. 1445–1461, 2021.
- [6] J. V. Aravind, S. Kumar, and S. Prince, "Performance analysis of uwoc using siso and simo techniques," *Journal of Physics: Conference Series*, vol. 1964, no. 6, p. 062025, jul 2021.
- [7] N. Watoniah, S. Pramono, and E. D. Wardihani, "Performance of mimo-ofdm systems in canal rayleigh," *JAICT*, vol. 4, no. 1, pp. 6–12, 2019.
- [8] G. Sharma and R. Sharma, "Performance comparison of centralised and distributed css over fading channels in cognitive radio," *Cogent Engineering*, vol. 4, no. 1, p. 1355599, 2017.
- [9] S. Mukherjee, S. S. Das, A. Chatterjee, and S. Chatterjee, "Analytical calculation of rician k-factor for indoor wireless channel models," *IEEE Access*, vol. 5, pp. 19 194–19 212, 2017.
- [10] P. Budhgaon, "Multipath fading channel modeling and performance comparison of wireless channel models," *International Journal of Electronics and Communication Engineering*, vol. 4, no. 2, p. 189, 2018.
- [11] K. Sunil, M. Sumithra, and M. Sarumathi Ms, "Performance analysis of rician fading channels using non-linear modulation methods with memory schemes in simulink environment," *IOSR Journal of Computer Engineering*, vol. 11, no. 4, pp. 27–36, 2013.
- [12] M. Mazid-Ul-Haque and M. S. Islam, "Data rate limit in low and high snr regime for nakagami-q fading wireless channel," *International Journal of Advanced Computer Science and Applications*, vol. 11, no. 7, 2020.
- [13] P. Cui, S. Han, X. Xu, J. Zhang, P. Zhang, and S. Ren, "End-to-end delay performance analysis of industrial internet of things: A stochastic network calculus perspective," *IEEE Internet of Things Journal*, vol. 11, no. 3, pp. 5374–5387, 2024.
- [14] P. Yadav, S. Kumar, and R. Kumar, "A review of transmission rate over wireless fading channels: Classifications, applications, and challenges," *Wireless Personal Communications*, vol. 122, no. 2, pp. 1709–1765, 2022.
- [15] O. Waqar, "Performance analysis for irs-aided communication systems with composite fading/shadowing direct link and discrete phase shifts," *Transactions on Emerging Telecommunications Technologies*, vol. 32, no. 10, p. e4320, 2021.
- [16] D. Krstic, P. Nikolic, S. Minic, and Z. Popovic, "Some performance of three-hop wireless relay channels in the presence of rician fading," in *The Sixteenth International Conference on Wireless and Mobile Communications ICWMC*, 2020, pp. 18–23.
- [17] P. Bapna, S. Joshi, and N. Kothari, "Path loss and fading characterization at 2.4 ghz for indoor scenario," *International Journal of Computer Applications*, vol. 975, p. 8887, 2019.
- [18] G. Zucca, M. Palmieri, and F. Cianetti, "On the statistical distribution of the maxima of sine on random process," *Mechanical Systems and Signal Processing*, vol. 158, p. 107726, 2021.
- [19] J. Wang, Y. Cui, H. Sun, X. Feng, G. Han, M. Wen, J. Li, and H. Esmaili, "K-factor estimation for wireless communications over rician frequency-flat fading channels," *IEEE Wireless Communications Letters*, vol. 10, no. 9, pp. 2037–2040, 2021.
- [20] D. L. Hall, M. J. Brandsema, and R. M. Narayanan, "Derivation of k-factor detection statistics to discriminate between los and nlos scenarios," *IEEE Transactions on Wireless Communications*, vol. 21, no. 4, pp. 2668–2679, 2022.
- [21] M. Richards, "Rice distribution for rcs," *Georgia Institute of Technology*, 2006.
- [22] N. O. Garzón, H. C. Mora, F. A. García, and C. D. Altamirano, "On the bit error probability and the spectral efficiency of opportunistic wireless transmissions in rician fading channels," *IEEE Access*, vol. 9, pp. 49 267–49 280, 2021.
- [23] S. B. Shawkat, M. Mazid-Ul-Haque, M. S. Islam, and B. S. Sonok, "Fundamental capacity analysis for identically independently distributed nakagami-q fading wireless communication," *International Journal of Advanced Computer Science and Applications*, vol. 11, no. 9, 2020.
- [24] D. S. Kapoor and A. K. Kohli, "Spatially-coded ofdm wireless systems employable in 5g communication networks—a review," vol. 29, no. 4, p. 10965–11003, 2020.
- [25] M. S. Islam and M. R. Islam, "Ergodic capacity of a simo system over nakagami-q fading channel," Ph.D. dissertation, DUET Journal, 2014.
- [26] B. S. Sonok, M. S. Islam, and M. Mazid-Ul-Haque, "Hoyt wireless fading channel capacity analysis using large limit argument approximation," in *Proceedings of the 2nd International Conference on Computing Advancements*, ser. ICCA '22. New York, NY, USA: Association for Computing Machinery, 2022, p. 18–24. [Online]. Available: <https://doi.org/10.1145/3542954.3542958>
- [27] W. R. Inc., "Mathematica, Version 14.0." champaign, IL, 2024.